# Light-Matter Correlation Energy Functional of the Cavity-Coupled Two-Dimensional Electron Gas via Quantum Monte Carlo Simulations

Lukas Weber,[1,2] Miguel A. Morales,[1] Johannes Flick,[1,3,4] Shiwei Zhang,[1] and Angel Rubio[2,1]
[1]Center for Computational Quantum Physics, The Flatiron Institute, 162 Fifth Avenue, New York, New York 10010, USA
[2]Max Planck Institute for the Structure and Dynamics of Matter, Luruper Chaussee 149, 22761 Hamburg, Germany
[3]Department of Physics, City College of New York, New York, New York 10031, USA
[4]Physics Program, Graduate Center, City University of New York, New York, New York 10016, USA

(Received 9 January 2025; revised 20 May 2025; accepted 28 August 2025; published 17 September 2025)

We perform extensive simulations of the two-dimensional cavity-coupled electron gas in a modulating potential as a minimal model for cavity quantum materials. These simulations are enabled by a newly developed quantum-electrodynamical (QED) auxiliary-field quantum Monte Carlo method. We present a procedure to greatly reduce finite-size effects in such calculations. Based on our results, we show that a modified version of weak-coupling perturbation theory is remarkably accurate for a large parameter region. We further provide a simple parametrization of the light-matter correlation energy as a functional of the cavity parameters and the electronic density. These results provide a crucial step toward a numerical foundation for the development of the QED density functional theory, which was previously reliant on analytical approximations, to allow quantitative modeling of a wide range of systems with light-matter coupling.

DOI: 10.1103/lq1y-q74h

In recent years, cavity quantum electrodynamics (QED) [1–5] has started to unveil its potential as a tool to modify not only chemical reactions [6–8] but also the properties of quantum matter [9,10]. These advances have created a demand for predictive numerical methods that can treat cavity photons and the constituents of matter on the same level. To satisfy this demand, extensions of existing electronic-structure methods have been developed, such as QED coupled-cluster methods [11–13], density-matrix renormalization group methods [14–16], and quantum Monte Carlo (QMC) methods, including the stochastic series expansion [17–19] and diffusion Monte Carlo method [20].

While the majority of these algorithms emphasize accurate computations for molecular or lattice-model systems, there is currently no comprehensive many-body approach for cavity-coupled bulk systems, in particular in the continuum. A promising candidate for *ab initio* calculations for such systems is the quantum-electrodynamical density functional theory (QEDFT) [1,21,22], which has seen tremendous progress in the development of light-matter exchange-correlation energy functionals. Progress in the development of these functionals has come from multiple approaches, including the optimized effective potential method [23], the fluctuation-dissipation theorem [24], the random-phase approximation [25], the many-body-dispersion method [26], or the photon-free approximation [27,28]. These functionals and their underlying approximations have been shown to work well in selected regimes of light-matter coupling or frequency. However, they still lack the foundation of generalizable and reliable numerical results covering the whole range of interactions, at a level comparable to the QMC solution of the electron gas [29] that originally enabled the success of purely electronic DFT [30].

In this Letter, we provide a crucial step toward this numerical foundation by applying the newly developed QED auxiliary-field quantum Monte Carlo (QED-AFQMC) method [31] to solve a minimal model for cavity quantum materials: the cavity-coupled two-dimensional electron gas in a soft modulating external potential [Fig. 1(a)]. After proposing a scheme to handle a class of finite-size effects that uniquely plague QED-coupled bulk systems, we obtain the light-matter correlation energy in the thermodynamic limit. For weak potentials, this energy is described well by a modified perturbation theory (PT). For the full range of parameters, we fit the correlation energy to a simple functional of the cavity parameters and the electronic density. These findings serve as both a benchmark for future cavity QED many-body methods and as a direct ingredient for the ongoing QEDFT functional development.

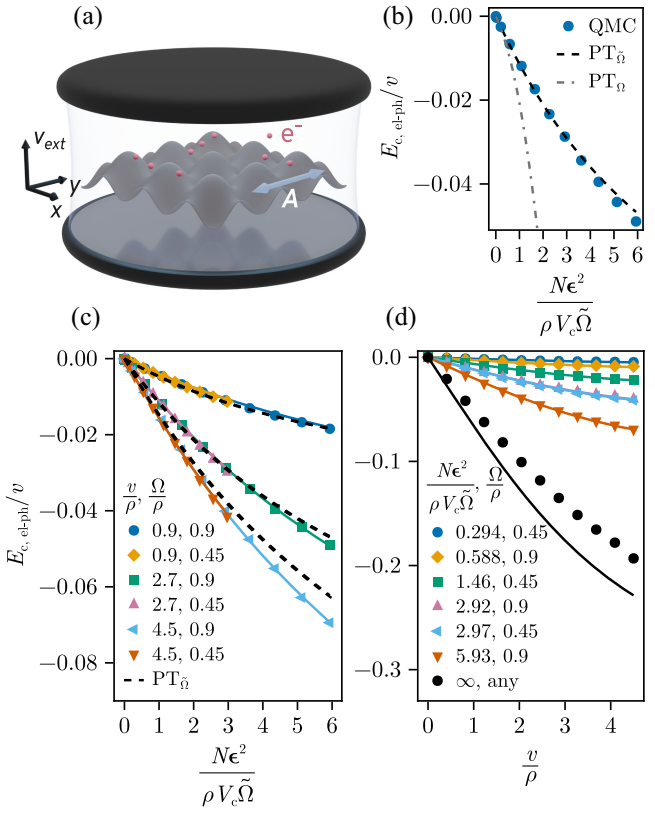


FIG. 1. Electron-photon correlation energy of the cavity-coupled electron gas in the modulated potential. (a) Sketch of the model with electron gas in a soft external potential $v_{\text{ext}}$. The polarization of the cavity mode is in one of the lattice directions. (b) The effectiveness of weak-coupling perturbation theory with $\tilde{\Omega} = \text{const}$ ($\text{PT}_{\tilde{\Omega}}$) compared to leaving $\Omega = \text{const}$ ($\text{PT}_{\Omega}$) and QMC data for $v/\rho = 2.7$ and $\Omega/\rho = 0.9$. (c),(d) Fit (solid lines) of the light-matter correlation energy $E_{\text{c,el-ph}}$ to slices of the parameter space, spanned by the average electron density $\rho = 1/a^2$, the potential depth $v$, the frequency $\Omega$, and the light-matter coupling $|\boldsymbol{\epsilon}|$. Black dashed lines correspond to the weak-coupling perturbation theory ($\text{PT}_{\tilde{\Omega}}$), while black circles are AFQMC results of the infinitely light-matter coupled asymptotic model, which was not included in the fit. The black solid line shows the extrapolation of the fit to infinite coupling. The error bars are smaller than the symbol size.

*Model*—We consider the Hamiltonian [32] of many electrons coupled to a single photon mode of frequency $\Omega$,

$$H = \sum_i \frac{(\mathbf{p}_i + \mathbf{A})^2}{2} + v_{\text{ext}}(\mathbf{r}_i) + \frac{\Omega}{2}\left(\Pi_{\text{ph}}^2 + Q_{\text{ph}}^2 - 1\right), \quad (1)$$

in two dimensions, where $\mathbf{A} = Q_{\text{ph}}\boldsymbol{\epsilon}/\sqrt{\Omega V_c}$, where $Q_{\text{ph}}$ ($\Pi_{\text{ph}}$) is the photon displacement (momentum) operator of the photon mode. We treat the model in the long-wavelength limit, with a position independent vectorial coupling $\boldsymbol{\epsilon}$ and a mode volume $V_c$, which we scale with the system size. Our method, which can treat realistic electronic interactions in periodic systems in the continuum at high accuracy [31,33], allows the incorporation of light and electron-light interaction on equal footing. In the first part of this Letter, we will not consider the Coulomb repulsion. Under this condition, our AFQMC simulations do not suffer from a phase problem [34] and are exact. At the end, we will briefly comment on the effect of including the Coulomb repulsion.

The cavity-coupled homogeneous electron gas ($v_{\text{ext}} = 0$), due to the conservation of the total momentum, can be solved exactly [35] by a product state between light and matter, $|\Psi_{\text{el}}\rangle \otimes |\chi_{\text{ph}}\rangle$, completely lacking any light-matter correlation. In a real material (with $v_{\text{ext}} \neq 0$), however, the crystal lattice breaks the perfect momentum conservation and induces momentum fluctuations that render the light-matter interaction nontrivial.

Therefore, for a true minimal model of cavity materials, we need to add an external potential to break the translation symmetry [Fig. 1(a)]. In this Letter, we choose a cosine potential $v_{\text{ext}}(\mathbf{r}) = -v\sum_{d=x,y}\cos[(2\pi\mathbf{e}_d/a)\cdot\mathbf{r}]$ with the potential depth $v$ and the lattice constant $a$. While this choice is primarily to keep the computational demand in our plane-wave-basis calculation manageable, it could in principle also be realized as a moiré potential [36].

*Toroidal magnetic finite-size effects*—When performing correlated calculations on finite systems, care has to be taken to correctly deal with finite-size effects. We find that light-matter coupled systems with periodic boundary conditions display a particular class of finite-size effect that—unless subtracted—dominates the effect of light-matter interactions on the energy in numerically accessible system sizes [Fig. 2(a)].

Considering our Hamiltonian from Eq. (1) with periodic boundary conditions, or equivalently, on a finite torus, the mode function of the cavity photon, albeit constant, wraps around the torus in one direction, realizing a finite magnetic flux loop. In finite systems with periodic boundary conditions, this can in general give rise to a symmetry broken ground state with $\langle\mathbf{A}\rangle \neq 0$ that describes a magnetic field induced by a circular current. Another way to interpret this phenomenon is to consider that a finite momentum space lattice breaks the gauge invariance of the model that would usually allow eliminating any finite expectation value of $\langle\mathbf{A}\rangle$ via a gauge transformation $\mathbf{p}_i \mapsto \mathbf{p}_i - \langle\mathbf{A}\rangle$. While these finite toroidal currents and fields have to vanish in the thermodynamic limit, they lead to strong energy contributions that can mask the signal of the light-matter correlation energy, making the proper extrapolation to the thermodynamic limit difficult [Fig. 2(b)].

We therefore propose a combination of two strategies to mitigate this problem. First, we define the light-matter correlation energy as $E_{\text{c,el-ph}} = E - E_{\text{CS}}$, where $E_{\text{CS}}$ is the best variational energy that can be achieved with a light-matter product state on the same finite system, explicitly allowing $\langle\mathbf{A}\rangle \neq 0$. Both terms of this difference display

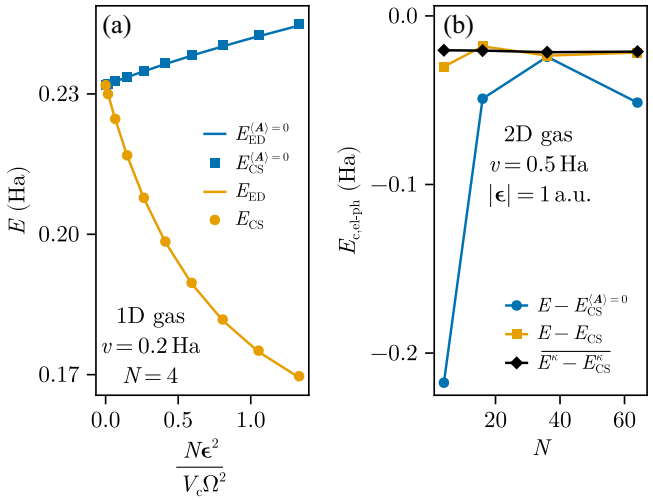


FIG. 2. Toroidal magnetic finite-size effects. In both panels, $a=3a_0$, $\Omega=0.05$ Ha, and $N=N_{\mathrm{uc}}$ is the number of electrons and unit cells. (a) The low-energy spectrum of the one-dimensional cavity-coupled electron gas computed with exact diagonalization. At finite light-matter coupling, the ground state $E_{\mathrm{ED}}$ is a doublet belonging to total crystal momentum $K=\pm 4\pi/L=\pm\pi/a$ (yellow circles) and correspondingly finite $\langle\mathbf{A}\rangle$. The first excited state $E_{\mathrm{ED}}^{\langle\mathbf{A}\rangle=0}$ is a doublet with $K=0$. The Hilbert space was constrained to 21 momenta and $n_{\mathrm{ph}}<20$, which is converged to the complete basis set limit. (b) A comparison of the finite-size scaling of the two-dimensional light-matter correlation energy derived from different subtraction schemes, obtained from AFQMC. $\overline{E^\kappa-E_{\mathrm{CS}}^\kappa}$ denotes the average over 60 twisted boundary conditions.

magnetic solutions, leading to a leading-order cancellation of the term $\langle\mathbf{P}_{\mathrm{tot}}\rangle\cdot\langle\mathbf{A}\rangle$ from the energy [Fig. 2(b)].

In the absence of Coulomb interactions, we can obtain $E_{\mathrm{CS}}$ by variationally minimizing the energy of a product state between a Slater determinant and a squeezed coherent state (CS): $|\Psi_{\mathrm{CS}}\rangle=|\psi_{\mathrm{el}}\rangle\otimes\int dq\sqrt[4]{(s/\pi)}e^{-s(q-q_0)^2/2}|q\rangle$ with the parameters $|\psi_{\mathrm{el}}\rangle$, $s$, and $q_0$. Under the assumption that the ground state is a pure light-matter product state, this ansatz solves Eq. (1) exactly, such as in the case $v=0$. We will further use this state as the trial wave function in our AFQMC calculations.

In addition to the introduction of this new definition of the correlation energy, we also employ twist-averaged boundary conditions [37]. These boundary conditions can be realized by quantizing the momenta in the $L\times L$ supercell as $\mathbf{k_n}=[2\pi/L](\mathbf{n}+\boldsymbol{\kappa})$ with a shift $\boldsymbol{\kappa}$ that lives in the square $\|\boldsymbol{\kappa}\|_\infty<\frac{1}{2}$ and then averaging the results over $\boldsymbol{\kappa}$. On top of being an established approach to reduce QED-unrelated finite-size effects [38], the average over $\boldsymbol{\kappa}$ formally restores gauge invariance, so that, e.g., the twist-averaged $\overline{\langle\mathbf{A}\rangle}$ or $\overline{\langle\mathbf{P}_{\mathrm{tot}}\rangle}$ vanish, and convergence with system size is vastly improved [Fig. 2(b)]. With this approach, we find sufficient convergence to the thermodynamic limit already at $N=4\times 4$ unit cells. To perform the twist average efficiently, we use quasirandom $\boldsymbol{\kappa}$ [38], chosen from the low-discrepancy Halton sequence [39]. An alternative way to eliminate the toroidal magnetic finite-size effects is to use closed boundary conditions [see Supplemental Material (SM) Sec. III [40]]. In this case, however, the scattering on the boundaries themselves leads to large finite-size effects, preventing an efficient extrapolation to the thermodynamic limit.

*Results*—In our calculations, we will consider supercells with one electron per $a\times a$ unit cell. We build a plane-wave basis consisting of the momenta $\mathbf{k_n}$ where we constrain the integer vector $\mathbf{n}$ to the smallest sphere that contains at least $fN_{\mathrm{uc}}$ momenta and average over 60 twist angles. For our $4\times 4$ supercell we find that $f=15$ is sufficient to converge to the complete basis set limit. We perform our AFQMC calculations at a time step of $\tau=0.01$ Ha$^{-1}$ with 300 walkers. We have verified that the residual systematic error from either of these parameters is smaller than our statistical error bars.

To map out the parameter space, we first identify the different energy scales in our model, namely the kinetic energy of the electrons, $E_{\mathrm{kin}}\sim\rho^{2/D}$ (in $D=2$ dimensions), with $\rho=1/a^2$ for one electron per unit cell, and the potential depth $v$, the renormalized cavity frequency $\tilde{\Omega}=\Omega\sqrt{1+N\epsilon^2/V_c\Omega^2}$, and the light-matter interaction scale $N\epsilon^2/V_c\tilde{\Omega}$. Note that the results can only depend on $\Omega$ through $\tilde{\Omega}$ as can be shown by absorbing the $\mathbf{A}^2$ term in a canonical transformation.

Using these energy scales, we can construct dimensionless ratios and write the light-matter correlation energy as

$$\frac{E_{\mathrm{c,el\text{-}ph}}}{\rho^{2/D}}=\mathcal{E}(x_v,x_\epsilon,x_{\tilde{\Omega}}),\tag{2}$$

with $x_v=\rho^{-2/D}v$, $x_\epsilon=\rho^{-2/D}N\epsilon^2/V_c\tilde{\Omega}$, and $x_{\tilde{\Omega}}=\rho^{-2/D}\tilde{\Omega}$. We will see later that this choice of variables already captures many features of $E_{\mathrm{c,el\text{-}ph}}$, leading to a simple functional form of $\mathcal{E}$.

We perform simulations of slices through this parameter space, along the direction of either $x_\epsilon$ [Fig. 1(c)] or $x_v$ [Fig. 1(d)]. For both $x_\epsilon=0$ or $x_v=0$, the correlation energy vanishes—the latter being consistent with the fact that for the homogeneous electron gas, the ground state is a light-matter product state. Conversely, for $x_\epsilon$ approaching infinity, the correlation energy approaches a bound given by an asymptotic infinite-coupling Hamiltonian,

$$\begin{aligned}H_\infty&=\lim_{|\boldsymbol{\epsilon}|\to\infty}U_{\mathrm{LF}}^\dagger H U_{\mathrm{LF}}\\&=\frac{1}{2}\sum_i[\mathbf{p}_i^2+v_{\mathrm{ext}}(\mathbf{r}_i)]-\frac{(\hat{\boldsymbol{\epsilon}}\cdot\mathbf{P}_{\mathrm{tot}})^2}{2N},\end{aligned}\tag{3}$$

with $\hat{\boldsymbol{\epsilon}}=\boldsymbol{\epsilon}/|\boldsymbol{\epsilon}|$, which follows from the Lang-Firsov transformation $U_{\mathrm{LF}}=\exp(i\Pi_{\mathrm{ph}}\boldsymbol{\epsilon}\cdot\mathbf{P}_{\mathrm{tot}}/\sqrt{V_c\tilde{\Omega}^3})$ (see SM Sec. I [40]).

This Hamiltonian can also be simulated exactly using a standard AFQMC calculation, and its correlation energy is shown in Fig. 1(d). The original photon-free functional [27] for QEDFT approximates the light-matter problem with a similar Hamiltonian. It has been shown to perform especially well in the strong-coupling regime. However, we find that convergence to the strong-coupling limit is in general slow, which explains why a functional based purely on a strong-coupling approximation does not generalize well to the weaker coupling regimes and can be improved by interpolating to a weak-coupling approximation [28].

We further compare our data to weak-coupling PT for the light-matter correlation energy, derived in SM Sec. I [40]:

$$E_{\mathrm{c,el\text{-}ph}}^{\mathrm{PT}_{\tilde{\Omega}}} = -\frac{1}{2V_c\tilde{\Omega}} \sum_{\substack{n\in \mathrm{occ} \\ m\notin \mathrm{occ}}} \frac{|\langle \psi_m^{\mathrm{el}}|\boldsymbol{\epsilon}\cdot\mathbf{p}|\psi_n^{\mathrm{el}}\rangle|^2}{\tilde{\Omega}+\varepsilon_m^{\mathrm{el}}-\varepsilon_n^{\mathrm{el}}}. \tag{4}$$

Here, $|\psi_n^{\mathrm{el}}\rangle$ and $\varepsilon_n^{\mathrm{el}}$ are the single-particle eigenstates and energies of the matter system (including spin), with the same twist-averaged boundary conditions as the other calculations, and $\mathbf{p}$ is the single-particle momentum. In our derivation we have left $\tilde{\Omega}$ intact, which we call $\mathrm{PT}_{\tilde{\Omega}}$. Alternatively one could expand $\tilde{\Omega} = \Omega + \mathcal{O}(\epsilon^2)$, which we call $\mathrm{PT}_{\Omega}$.

Figures 1(b) and 1(c) show that while $\mathrm{PT}_{\Omega}$ is only valid for small light-matter coupling, $\mathrm{PT}_{\tilde{\Omega}}$ is remarkably accurate to very large couplings, as long as $x_v$ is not too large. In earlier calculations in the velocity gauge, $\mathrm{PT}_{\tilde{\Omega}}$ has been a natural choice [28,44], but this choice is much less obvious in the dipole gauge. Because of the gauge invariance of the perturbation theory, it may be possible to simply replace $\Omega = \tilde{\Omega}\sqrt{1-N\epsilon^2/V_c\tilde{\Omega}^2}$ in the dipole-gauge Hamiltonian to significantly enhance dipole-gauge perturbative calculations.

Our next goal is to find a simple analytical expression for $\mathcal{E}$ as a functional of the electron density and the cavity parameters that fits our numerical data well. To this end, we must first eliminate the explicit dependence on $x_v$. Since the photon only sees the spatially integrated effect of the momentum fluctuations caused by the potential, it is expected that the average of the squared gradient of the density $n(\mathbf{r})$ in the polarization direction, $\mathcal{Q}^2 = \{\int dV[\hat{\boldsymbol{\epsilon}}\cdot\nabla n(\mathbf{r})]^2 / \int dV[n(\mathbf{r})]^2\}$, is a good proxy for the effect of $x_v$ that is well defined both in infinite periodic and finite molecular systems.

Next, we want to determine the dimensionless function $x_q(x_v) = \mathcal{Q}^2/\rho^{2/D}$. Since in our extended system, electronic quantities are not affected by the intensive contribution of the photons, we can calculate this quantity in the pure matter system. Based on asymptotic analysis of the $v \ll \rho$ and $v \gg \rho$ limits and a fit, we find the Padé-like interpolant $x_q(x_v) = x_v^2/(b_1 + b_2 x_v + b_3 x_v^{3/2})$, with $b_1 = 3.27$, $b_2 = -0.242$, and $b_3 = 0.213$, to accurately describe all systems treated in the QMC simulations (see SM Sec. II [40]).

Having found a proxy for the $x_v$ dependence, the next step is to come up with a fitting function $\mathcal{E}(x_q, x_\epsilon, x_{\tilde{\Omega}})$. A first helpful observation is that the parameter $x_{\tilde{\Omega}}$ barely contributes at fixed $x_v$ and $x_\epsilon$ [Fig. 1(c)]. This is not surprising since $x_{\tilde{\Omega}} \longrightarrow^{x_\epsilon\to\infty} x_\epsilon$. Additionally, we can take advantage of the asymptotics of the perturbative solutions for weak coupling, $\mathcal{E} \overset{x_\epsilon\to 0}{\sim} x_\epsilon x_q$, and strong coupling, $\mathcal{E} \overset{x_\epsilon\to\infty}{\sim} \mathcal{E}(x_q)$. We propose a simple rational function $\mathcal{E}(x_v, x_\epsilon) = -(x_\epsilon x_q/c_1 x_\epsilon + c_2)$ that fulfills these criteria and has two parameters we fit to the data from Figs. 1(c) and 1(d). While it is possible to also include the $|\boldsymbol{\epsilon}| = \infty$ data in the fit, for the sake of simplicity of the functional and accuracy at realistic couplings, we only fit to finite coupling, where our maximum deviation from the data is 0.4 mHa. Nevertheless, our functional still extrapolates qualitatively correctly to the infinite-coupling case [Fig. 1(d)].

Reexpressing in the dimensionful quantities, we arrive at the functional

$$E_{\mathrm{c,el\text{-}ph}} \approx -\frac{\mathcal{Q}^2}{c_1 + c_2\rho^{2/D}\frac{V_c\tilde{\Omega}}{N\epsilon^2}}, \tag{5}$$

with the fit parameters $c_1 = 4.672$, $c_2 = 63.73$. The corresponding real-space energy density per electron can be written as $e_{\mathrm{c,el\text{-}ph}}(\mathbf{r}) = -[\hat{\boldsymbol{\epsilon}}\cdot\nabla n(\mathbf{r})]^2/[n(\mathbf{r})[c_1 + c_2\rho^{2/D} \times (V_c\tilde{\Omega}/N\epsilon^2)] \int dV' n^2(\mathbf{r}')]$.

*Effect of Coulomb repulsion*—In addition to the results above, we performed calculations that include the longitudinal Coulomb repulsion (Fig. 3). While comprehensive

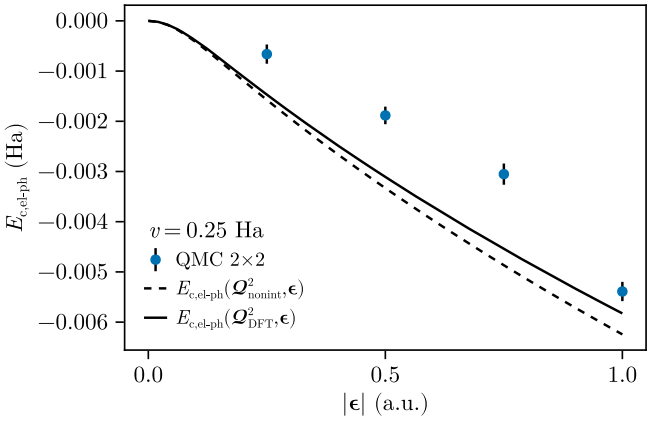


FIG. 3. The light-matter correlation energy $E_{\mathrm{c,el\text{-}ph}}$ of the cavity-coupled Coulomb interacting electron gas in a modulating potential as a function of the light-matter coupling $|\boldsymbol{\epsilon}|$. In addition to the AFQMC results, results from the non-Coulomb-interacting light-matter correlation energy functional with noninteracting density and density obtained from a single-shot DFT calculation are shown.

parameter scans are challenging, and different sources of uncertainty, including finite-size effects, remain (see SM Sec. IV [40]), we find that (although the overall correlation energy increases) the repulsion leads to a decrease in light-matter correlation energy. This decrease can be qualitatively explained using our functional and the repulsion-induced smoothing of the electronic density. It is likely that the functional needs to be extended to include a dependency on an additional Coulomb-related scale.

*Conclusion*—We have performed high-accuracy AFQMC simulations for the cavity-coupled two-dimensional electron gas in a modulating external potential. As a first step, we study the system without Coulomb interactions and with a single photon mode in the long-wavelength approximation. After dealing with a class of magnetic finite-size effects that uniquely affect cavity-coupled systems on finite tori, we extract the light-matter correlation energy, scanning the model parameter space including the full range of light-matter couplings. Finally we provide a parametrization of this energy, in terms of the light-matter coupling, the cavity frequency, the density, and the density gradient.

When interpreting these results, it is important to consider the properties of the actual cavity setup, which, given its finite finesse, can couple only a finite volume of matter coherently [45]. This maximum volume cuts off the notion of an infinite system size thermodynamic limit, and the effect of the light-matter correlations presented here should always be put into relation with a finite system smaller than that volume. For a system larger than the maximum volume, the finite coherence length of the cavity photons has to be taken into account. For very short coherence lengths of the order of a few unit cells, the supercell extrapolation in the present Letter would also be cut off. In such cases, a full minimal-coupling treatment is likely necessary. The cavity properties also determine the realistic values for $x_\epsilon$. To resolve the crossover to the $x_\epsilon \to \infty$ limit, we simulated parameter sets deep into the diamagnetic regime $\tilde{\Omega}/\Omega \gg 1$, whereas realistic values for $x_\epsilon$ for many materials and cavities may be much smaller. More detailed investigations of the small $x_\epsilon$ regime are left for future work.

Apart from the energy functional itself, we find that for the given Hamiltonian, the weak-coupling perturbation theory at constant renormalized frequency $\tilde{\Omega}$, as opposed to the perturbation theory that uses the bare frequency, is remarkably effective at describing our data. This provides a key many-body benchmark for future studies. We expect that existing perturbative functionals, in particular those in the dipole gauge, can be improved by treating $\tilde{\Omega}$ as a constant during the expansion. Further, we find that the infinite-coupling limit is a well-defined model with a finite light-matter correlation energy, albeit this limit is approached rather slowly.

While a complete inclusion of Coulomb interactions in the reference data was beyond the scope of this Letter, we benchmark our functional on a range of Coulomb interacting systems. The reduction of the light-matter correlation energy we find can be explained qualitatively by our functional, but remaining quantitative differences suggest the importance of treating transversal and longitudinal interactions on the same footing. This extension, and other next steps, such as the extension to three-dimensions and multiple mode, are all within reach of our AFQMC method, and left for future work toward a general functional for *ab initio* QED material calculations.

Beyond the implications for QEDFT, our Letter also highlights the viability of QED-AFQMC itself as a tool for simulating cavity-coupled bulk systems, which is of particular interest for scenarios where both electron-photon and electron-electron correlations are significant.

The Monte Carlo simulations are based on the Carlo.jl [46] framework. We used Optim.jl [47] and Zygote.jl [48] for optimizing our trial wave functions and Makie.jl [49] for creating the figures.

*Acknowledgments*—We thank Michael Ruggenthaler, Mark Kamper Svendsen, Martin Claassen, Christian Eckhardt, Daniele Guerci, and I-Te Lu for fruitful discussions. L. W. acknowledges support by the Deutsche Forschungsgemeinschaft (DFG, German Research Foundation) through Grant No. WE 7176-1-1. The Flatiron Institute is a division of the Simons Foundation.

*Data availability*—The data that support the findings of this article are openly available [50].

[1] M. Ruggenthaler, J. Flick, C. Pellegrini, H. Appel, I. V. Tokatly, and A. Rubio, Quantum-electrodynamical density-functional theory: Bridging quantum optics and electronic-structure theory, Phys. Rev. A **90**, 012508 (2014).

[2] H. Hübener, U. De Giovannini, C. Schäfer, J. Andberger, M. Ruggenthaler, J. Faist, and A. Rubio, Engineering quantum materials with chiral optical cavities, Nat. Mater. **20**, 438 (2020).

[3] F. Schlawin, D. M. Kennes, and M. A. Sentef, Cavity quantum materials, Appl. Phys. Rev. **9**, 011312 (2022).

[4] H. Hübener, E. Boström, M. Claassen, S. Latini, and A. Rubio, Quantum materials engineering by structured cavity vacuum fluctuations, Mater. Quantum Technol. **4**, 023002 (2024).

[5] M. Ruggenthaler, D. Sidler, and A. Rubio, Understanding polaritonic chemistry from ab initio quantum electrodynamics, arXiv:2211.04241.

[6] A. Thomas, L. Lethuillier-Karl, K. Nagarajan, R. M. A. Vergauwe, J. George, T. Chervy, A. Shalabney, E. Devaux, C. Genet, J. Moran, and T. W. Ebbesen, Tilting a ground-state reactivity landscape by vibrational strong coupling, Science **363**, 615 (2019).

[7] W. Ahn, J. F. Triana, F. Recabal, F. Herrera, and B. S. Simpkins, Modification of ground-state chemical reactivity via light–matter coherence in infrared cavities, Science **380**, 1165 (2023).

[8] T. Ebbesen, A. Rubio, and G. Scholes, Introduction: Polaritonic chemistry, Chem. Rev. **123**, 12037 (2023).

[9] F. Appugliese, J. Enkner, G. L. Paravicini-Bagliani, M. Beck, C. Reichl, W. Wegscheider, G. Scalari, C. Ciuti, and J. Faist, Breakdown of topological protection by cavity vacuum fields in the integer quantum Hall effect, Science **375**, 1030 (2022).

[10] G. Jarc, S. Y. Mathengattil, A. Montanaro, F. Giusti, E. M. Rigoni, R. Sergo, F. Fassioli, S. Winnerl, S. Dal Zilio, D. Mihailovic, P. Prelovšek, M. Eckstein, and D. Fausti, Cavity-mediated thermal control of metal-to-insulator transition in 1T-$TaS_2$, Nature (London) **622**, 487 (2023).

[11] T. S. Haugland, E. Ronca, E. F. Kjønstad, A. Rubio, and H. Koch, Coupled cluster theory for molecular polaritons: Changing ground and excited states, Phys. Rev. X **10**, 041043 (2020).

[12] F. Pavošević and J. Flick, Polaritonic unitary coupled cluster for quantum computations, J. Phys. Chem. Lett. **12**, 9100 (2021).

[13] F. Pavošević, R. L. Smith, and A. Rubio, Computational study on the catalytic control of endo/exo Diels-Alder reactions by cavity quantum vacuum fluctuations, Nat. Commun. **14**, 2766 (2023).

[14] C. J. Eckhardt, G. Passetti, M. Othman, C. Karrasch, F. Cavaliere, M. A. Sentef, and D. M. Kennes, Quantum Floquet engineering with an exactly solvable tight-binding chain in a cavity, Commun. Phys. **5**, 122 (2022).

[15] G. Passetti, C. J. Eckhardt, M. A. Sentef, and D. M. Kennes, Cavity light-matter entanglement through quantum fluctuations, Phys. Rev. Lett. **131**, 023601 (2023).

[16] D. Shaffer, M. Claassen, A. Srivastava, and L. H. Santos, Entanglement and topology in Su-Schrieffer-Heeger cavity quantum electrodynamics, Phys. Rev. B **109**, 155160 (2024).

[17] L. Weber, E. Viñas Boström, M. Claassen, A. Rubio, and D. M. Kennes, Cavity-renormalized quantum criticality in a honeycomb bilayer antiferromagnet, Commun. Phys. **6**, 1 (2023).

[18] M. Weber, Quantum Monte Carlo simulation of spin-boson models using wormhole updates, Phys. Rev. B **105**, 165129 (2022).

[19] A. Langheld, M. Hörmann, and K. P. Schmidt, Quantum phase diagrams of Dicke-Ising models by a wormhole algorithm, arXiv:2409.15082.

[20] B. M. Weight, S. Tretiak, and Y. Zhang, Diffusion quantum Monte Carlo approach to the polaritonic ground state, Phys. Rev. A **109**, 032804 (2024).

[21] I. V. Tokatly, Time-dependent density functional theory for many-electron systems interacting with cavity photons, Phys. Rev. Lett. **110**, 233001 (2013).

[22] J. Flick, M. Ruggenthaler, H. Appel, and A. Rubio, Kohn–Sham approach to quantum electrodynamical density-functional theory: Exact time-dependent effective potentials in real space, Proc. Natl. Acad. Sci. U.S.A. **112**, 15285 (2015).

[23] C. Pellegrini, Optimized effective potential for quantum electrodynamical time-dependent density functional theory, Phys. Rev. Lett. **115**, 093001 (2015).

[24] J. Flick, Simple exchange-correlation energy functionals for strongly coupled light-matter systems based on the fluctuation-dissipation theorem, Phys. Rev. Lett. **129**, 143201 (2022).

[25] D. Novokreschenov, A. Kudlis, I. Iorsh, and I. V. Tokatly, Quantum electrodynamical density functional theory for generalized Dicke model, Phys. Rev. B **108**, 235424 (2023).

[26] C. Tasci, L. A. Cunha, and J. Flick, Photon many-body dispersion: An exchange-correlation functional for strongly coupled light-matter systems, arXiv:2404.04765.

[27] C. Schäfer, F. Buchholz, M. Penz, M. Ruggenthaler, and A. Rubio, Making *ab initio* QED functional(s): Nonperturbative and photon-free effective frameworks for strong light–matter coupling, Proc. Natl. Acad. Sci. U.S.A. **118**, e2110464118 (2021).

[28] I.-Te Lu, M. Ruggenthaler, N. Tancogne-Dejean, S. Latini, M. Penz, and A. Rubio, Electron-photon exchange-correlation approximation for quantum-electrodynamical density-functional theory, Phys. Rev. A **109**, 052823 (2024).

[29] D. M. Ceperley and B. J. Alder, Ground state of the electron gas by a stochastic method, Phys. Rev. Lett. **45**, 566 (1980).

[30] J. P. Perdew and A. Zunger, Self-interaction correction to density-functional approximations for many-electron systems, Phys. Rev. B **23**, 5048 (1981).

[31] L. Weber, L. dos Anjos Cunha, M. A. Morales, A. Rubio, and S. Zhang, Phaseless auxiliary-field quantum Monte Carlo method for cavity-QED matter systems, J. Chem. Theory Comput. **21**, 2909 (2025).

[32] C. Cohen-Tannoudji, J. Dupont-Roc, and G. Grynberg, *Photons and Atoms: Introduction to Quantum Electrodynamics* (John Wiley & Sons, Ltd., New York, 1997).

[33] M. Motta and S. Zhang, Ab initio computations of molecular systems by the auxiliary-field quantum Monte Carlo method, WIREs Comput. Mol. Sci. **8**, e1364 (2018).

[34] S. Zhang and H. Krakauer, Quantum Monte Carlo method using phase-free random walks with Slater determinants, Phys. Rev. Lett. **90**, 136401 (2003).

[35] V. Rokaj, M. Ruggenthaler, F. G. Eich, and A. Rubio, Free electron gas in cavity quantum electrodynamics, Phys. Rev. Res. **4**, 013012 (2022).

[36] S. Zhang *et al.*, Moiré superlattices in twisted two-dimensional halide perovskites, Nat. Mater. **23**, 1222 (2024).

[37] C. Lin, F. H. Zong, and D. M. Ceperley, Twist-averaged boundary conditions in continuum quantum Monte Carlo algorithms, Phys. Rev. E **64**, 016702 (2001).

[38] M. Qin, H. Shi, and S. Zhang, Benchmark study of the two-dimensional Hubbard model with auxiliary-field quantum Monte Carlo method, Phys. Rev. B **94**, 085103 (2016).

[39] J. H. Halton, On the efficiency of certain quasi-random sequences of points in evaluating multi-dimensional integrals, Numer. Math. **2**, 84 (1960).

[40] See Supplemental Material at http://link.aps.org/supplemental/10.1103/lq1y-q74h for derivations of the low- and high-coupling perturbative expressions and asymptotic behavior of $\mathcal{Q}^2$, which includes Refs. [41–43].

[41] M. Suewattana, W. Purwanto, S. Zhang, H. Krakauer, and E. J. Walter, Phaseless auxiliary-field quantum Monte Carlo calculations with plane waves and pseudopotentials: Aapplications to atoms and molecules, Phys. Rev. B **75**, 245123 (2007).

[42] C. Attaccalite, S. Moroni, P. Gori-Giorgi, and G. B. Bachelet, Correlation energy and spin polarization in the 2D electron gas, Phys. Rev. Lett. **88**, 256601 (2002).
[43] M. F. Herbst, A. Levitt, and E. Cances, DFTK: The density-functional toolkit, https://dftk.org/.
[44] N. Rivera, J. Flick, and P. Narang, Variational theory of nonrelativistic quantum electrodynamics, Phys. Rev. Lett. **122**, 193603 (2019).
[45] M. K. Svendsen, M. Ruggenthaler, H. Hübener, C. Schäfer, M. Eckstein, A. Rubio, and S. Latini, Theory of quantum light-matter interaction in cavities: Extended systems and the long wavelength approximation, arXiv:2312.17374.
[46] L. Weber, Carlo.Jl: A general framework for Monte Carlo simulations in Julia, SciPost Phys. Codebases **49** (2025)..
[47] P. K. Mogensen and A. N. Riseth, Optim: A mathematical optimization package for Julia, J. Open Source Software **3**, 615 (2018).
[48] M. Innes, Don't unroll adjoint: Differentiating SSA-form programs, arXiv:1810.07951.
[49] S. Danisch and J. Krumbiegel, Makie.jl: Flexible high-performance data visualization for Julia, J. Open Source Software **6**, 3349 (2021).
[50] L. Weber, M. A. Morales, J. Flick, S. Zhang, and A. Rubio, lukas-weber/qed-electron-gas-data: v1.0.0, 10.5281/zenodo.14611191 (2025).